A. Facilities in Operation

1. Beam Swinger Facility

An additional large detector hut was constructed so that large detector arrays (up to 1 1/2 meter by 1 1/2 meter x 1/10 meter) could be used on each of the three neutron flight lines (0° to 26°, 24° to 50° and 45° to 71°). Additional shielding was placed around the beam swinger Faraday cup to reduce background for the radiative np capture experiment of Meyer et al. A hoist for positioning a liquid hydrogen target just downstream of the swinger target area was installed for this experiment as well. A gas cell has been designed for use on the standard target ladder. This cell will be used in early 1982.

2. QQSP Pion Spectrometer

As discussed in the previous annual report, the magnetic fields of the QQSP quadrupoles were found to deviate significantly from their design values. Also some vertical misalignments were found. This past year the quadrupoles have been "reworked" to bring them closer to the design field values as well as realigned with additional support structures added to maintain the alignment. Restrictive quadrupole magnet vacuum chambers were modified and a number of additional system modifications were made in order to enhance the convenience of using and the performance of the QQSP. Following these repairs, additional raytracing with low energy protons showed that the previously measured vertical cutoff in solid angle had been remedied and that the QQSP was ready for experimental use (Fig. 3).

Other improvements to the QQSP system include:

1) A portable vacuum pumping station for the beam line to the QQSP beam dump. This pumping station allowed the dump to be better shielded, thereby reducing background at the QQSP detector position.

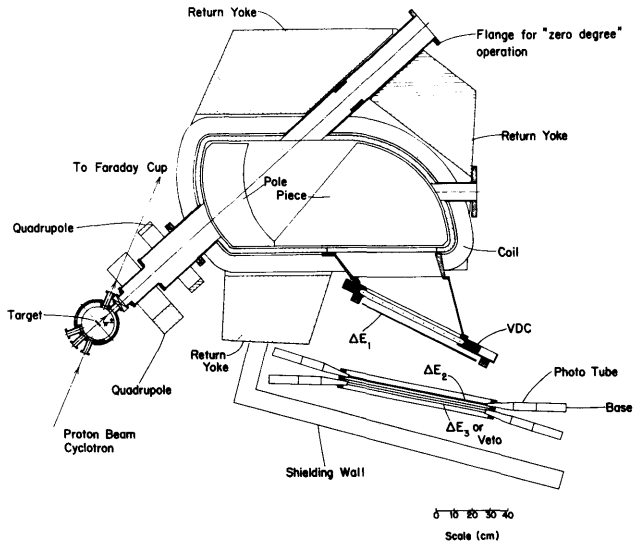

Figure 3. Layout of the pion spectrometer (QQSP) system showing the location of the detectors used in normal operations.

2) Smaller entrance and exit vacuum pipes and modified water lines and magnet leads to extend the angular range as far as possible.

3) Careful repositioning of the scattering chamber at the center of rotation of the spectrometer was accomplished in order to reduce undesirable stress on the sliding band seal of the QQSP. Currently, flexible water lines to the spectrometer are being replaced with rotatable water fittings in order to improve QQSP operation through its full angular range. In the late summer and early fall of 1981 more than 40 experimental shifts were used in the successful measurement of the $(p,\pi^{\pm})$ cross section and analyzing power angular distributions for the $^{12,13,14}C$ isotopes for T_p = 170, 180 and 190 MeV.[1] Shown in Fig. 4 is a typical $^{12}C(p,\pi^{+})^{13}C$ spectrum after software correction for QQSP aberrations and kinematic effects. All of the known states up to 9.5 MeV in ^{13}C have been labeled. The 100 keV FWHM resolution corresponds to a 2 mm

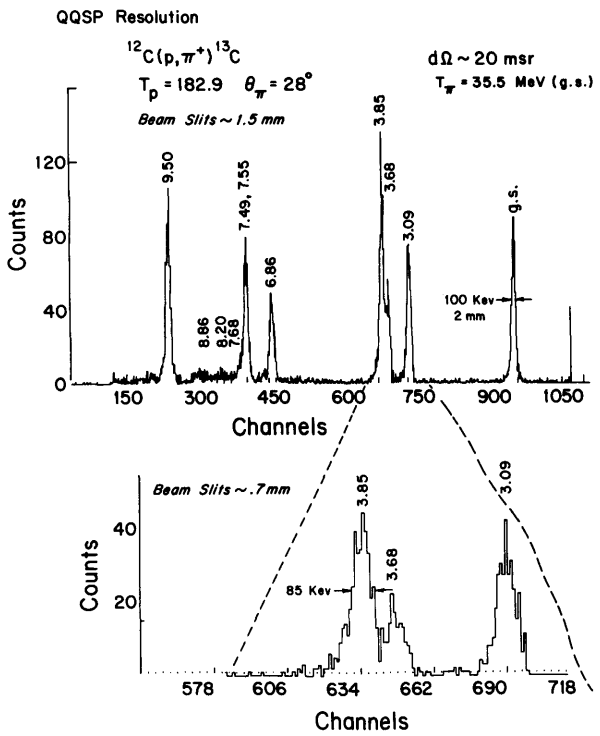

Figure 4. Excitation energy spectrum obtained for the $^{12}C(p,\pi^+)^{13}C$ reaction using the QQSP system. The overall resolution obtained was approximately 100 keV (FWHM).

displacement along the focal plane. The design goal for the QQSP magnet optics after software correction was 1 mm (FWHM), and intrinsic resolution of the VDC has been measured to be ~0.5 mm. We believe that the resolution measured so far has been limited by the energy distribution of the incident proton beam. Shown in the lower half of Fig. 4 is the 3-4 MeV excitation region for the same reaction. Here, the image and object slits of the beam analyzing magnet have been reduced by 50%. Some increase in resolution (FWHM ~85 keV) is seen but this gain is at the expense of beam intensity which was reduced by more than 75% in this case.

The QQSP spectrometer is now a fully operational experimental facility at IUCF. Documentation on the experimental setup exists and will soon be available as an internal report.

1) M.C. Green, "Recent Developments and Results in $(p,\pi^{\pm})$ at IUCF", AIP Conf. Proc. No. 79, Pion Production and Absorption in Nuclei (IUCF), Ed. R.D. Bent

3. QDDM Magnetic Spectrometer

A downstream scintillator was located in the QDDM scattering chamber to allow focussing of the beam past the target position. This procedure results in improved spectrometer resolution. Tests were performed which showed that the external Faraday cup (located 7m downstream from the target) is slightly misaligned. This misalignment can cause incomplete (by the order of 10%) charge collection in the Faraday cup for deuterons and other heavier particle beams especially with thick targets where multiple scattering is large. Realignment of this Faraday cup is planned for mid-1982. In order to accommodate improvements in the focal plane polarimeter used to measure spin-flip probabilities, a special interface vacuum box for the QDDM was designed, fabricated and operated. A design has been completed for a shorter permanent interface box which will allow the focal plane detectors to be placed at different angles by the use of smaller interface adaptors. There are indications that this capability will lead to improved spectrometer resolution. These parts will be fabricated by mid-1982.

A special target chamber was positioned just downstream of the QDDM scattering chamber to carry out (p,pn) measurements using a high-purity germanium telescope and large neutron detectors. Shielding wall blocks at the northeast corner of the QDDM vault were moved to provide sufficient distance for the neutron time-of-flight measurements involved.

4. 64" Scattering Chamber

The target table drive mechanism for this general purpose scattering chamber was redesigned and

implemented. Increased reliability (and ease of repair) of this mechanism was achieved. A special ring-shaped detector mount adaptor plate was fabricated and mounted to one arm of the chamber to accommodate the multi-detector array of the Maryland group. A variety of small detector adaptor parts were designed, fabricated and installed to allow the use of of other non-standard detector configurations including channel plate detectors.

5. Other Target Area and Support Efforts

Many small jobs are performed throughout the year to support the research efforts of the scientific user. For instance, a low beam intensity current monitor using scattered beam particles detected in a scintillator was built and made to work to support the ITT test of image dissectors. A rudimentary positioning device for supporting their dissectors in the beam was provided as well. Another example was the extemporization of several support structures for tests of multiwire proportional wire chambers and multichamber liquid scintillator detectors to be used in the CSB experiment. These supports had to be adjustable in several directions and were expected to be used only once.

Smaller jobs such as these together with routine reconfiguration of apparatus, changing power supply connections, and maintenance of existing equipment more than fill the available time between larger jobs such as installation of new permanent facilities and major improvements and modifications of existing equipment. The challenge of research support continues to grow and takes an increasingly large component of the laboratory's efforts.

6. Target and Detector Development

(i) Liquid Hydrogen and Deuterium Target Facility

A liquid hydrogen target has been constructed for use with Exp. 93 (radiative np capture). Its basic design and main components will be adapted to provide the new polarized neutron beam line with a deuterium production target. The first liquifaction of hydrogen was achieved in October 1981; the target in its final configuration became operational in January 1982.

The actual target cell as shown in Fig. 5 consists of a cylindrical stainless steel tube (1) with front and rear Mylar caps (2). The volume of the target is

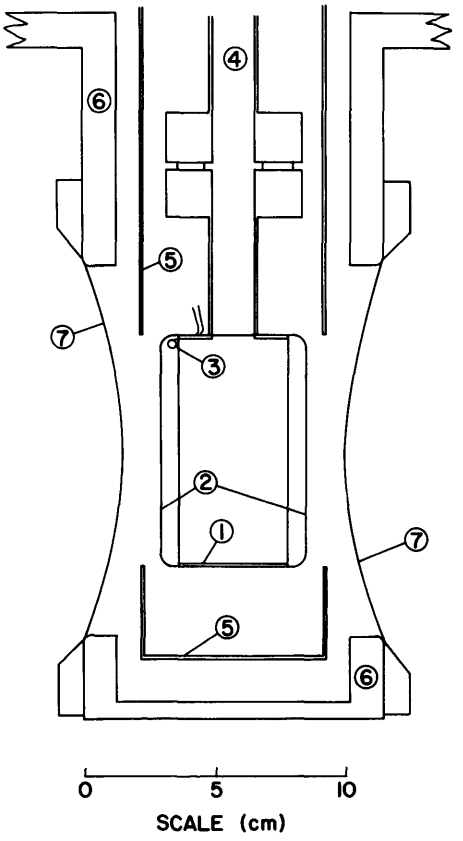

Figure 5. Cross section view of the liquid hydrogen target cell.

340 cm^3. The Mylar caps are made from flat Mylar sheets (≈.15 mm thick) heated to about 150°C, then extruded in a hot captive die and allowed to cool while still held by the die. The Mylar caps are joined to the stainless steel cylinder using Ecobond no. 285 epoxy with 24LV hardener. Several 1kΩ, 1/8W carbon resistors (3) serve to monitor the liquid level in the

target cell during operation. The electrical connections are fed through the thin layer of epoxy between the Mylar cap and the steel band. When the cell is filled with liquid H_2, an incident particle beam, parallel to the axis of the cylinder, passes through 0.4 g/cm^2 H_2.

The condensor/recondensor system (CTI Compressor Model #1020R and condensor/recondensor CTl Model #1023) is coupled to the target by a flanged 2cm disk stainless steel tube. The flanges use concentric point-to-point V grooves biting into an annealed copper ring to make a seal. This method allows easy change of target cells. The target and recondensor are wrapped with 3-4 layers of super insulation (not shown in Fig. 5) and surrounded by an 80 K radiation shield (5) coupled to the first stage of the condensor. The whole assembly is contained in a vacuum enclosure (6) with Mylar windows, 0.18mm thick (7) for beam entrance and exit. The pumping is provided by an air cooled 2-inch diffusion pump. The gas handling system features remotely operated valves and liguid nitrogen and chemical traps for purification of the hydrogen gas Since seven times more energy has to be removed in cooling down the H_2 from room temperature to 70°K than for liquifaction, the gas is precooled to liquid nitrogen temperature before it enters the condenser. Another important feature of the gas system is a storage tank of 300 ℓ capacity. This corresponds to the amount of liquid H_2 contained in the target cell at standard temperature and pressure. The storage tank holds the target gas when the unit is not in operation (especially necessary in the case of D_2), and also functions as a safety device.

During normal operation of the target, the cooling power of the compressor (~10W at 20°K) needs to be reduced substantially. If this is not done, H_2 will solidify at 14°K. An attempt was made to control the cooling power by actually regulating the coolant (^{4}He) pressure. It was found, however, that simply dissipating the excess cooling power by means of a heat load (carbon resistor), thermally connected to the cold part of the condenser, is to be preferred. If this heat load is operated with constant current, the temperature of the device is stabilized reliably, due to the strong temperature dependence of carbon resistors near and below 20°K.

There are three levels of safety precautions. H_2 is prevented from leaving the system, under almost all possible conditions. This is accomplished by the use of the storage tank which is automatically connected to the target cell if either the H_2 vapor pressure in the cell becomes too large or the surrounding vacuum pressure exceeds a preset value. This connection is also established if all AC power fails. This way, the pressure in the target stays safely below rupture pressure, even if the whole system is warmed to room temperature. The second safety level deals with the unlikely event of hydrogen gas escaping to the outside. A tent encloses the target assembly in order to confine any free H_2. The confined space is connected to a vent system with a forced gas flow of ~25 m^3/min. The fan of the system is explosion proof and is driven by 12V and 24V DC from a battery bank, thus ensuring operation with the building power off. All mechanical pumps are also vented into this vent system. In addition, at strategic places in the building, the H_2 level is monitored electronically. The third safety level, finally, concerns the event of an explosion. Here, we are determined to prevent injuries to personnel by following a strict safety code, making sure that the equipment is operated remotely from a place which is adequately shielded.

The liquid hydrogen target described here (filled with deuterium) will be used to produce neutrons via the $D(\vec{p},\vec{n})$ reaction in the polarized neutron beamline, presently under construction at IUCF. Necessary modifications of the present design include:
(i) different target cell and heat shield geometry,
(ii) an outer vacuum enclosure which provides vertical motion of the cell with respect to the beam axis,
(iii) a regulating feedback system to compensate for the varying heat load of the proton beam on the cryosystem and (iv) integration of the vacuum surrounding the target into the beam line vacuum system.

(ii) Liquid Scintillator Neutron Detectors

For experiment #80 ("Search for Charge Symmetry Violation in n-p Scattering," see refs. 1 and 2), we are constructing two large-volume, position-sensitive liquid scintillator detectors for medium-energy neutrons. The scintillating material (NE235H mineral-oil-based liquid) for each detector is contained in a large (1.41m x 1.22m x 0.42m) aluminum box. A system of interlaced reflecting walls (constructed from 0.1 cm thick highly polished aluminum) divides the active scintillator volume into 104 (13 columns x 8 rows) optically isolated subcells, each tapered and aimed at the target position (1.6m from the front face of the detector), subtending ±1.4° horizontally and ±1.8° vertically. Each subcell is viewed by an independent RCA 4518 (2-inch diameter, 10-stage) photomultiplier tube. Signals from each phototube are processed in a base incorporating a constant-fraction discriminator circuit in addition to the voltage divider resistor chain. We have chosen this "honeycomb" structure over other designs considered for the neutron detectors because of its relatively low construction cost and its logical simplicity. Position information for the neutron in this scheme is reduced to digital information (indicating which subcell fired), analogous to that provided for charged particles by multi-wire proportional chambers, thereby eliminating certain types of systematic errors which might otherwise result from drifts in analog electronics.

We have already completed the construction and successful testing[2] of a 12-cell prototype of the large neutron detectors (see Fig. 6), as well as the mechanical design of the large detectors and the acquisition of sufficient quantities of liquid scintillator, photomultiplier tubes, multi-channel high voltage power supplies, and highly polished aluminum for the construction of the large detectors. The base circuits have been designed and built by collaborators

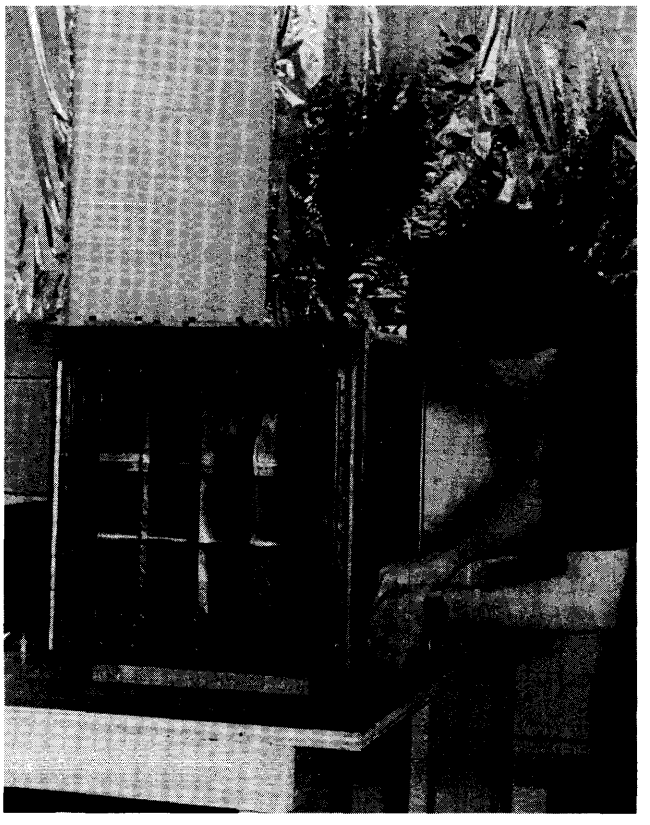

Figure 6. The 12-cell prototype neutron detector filled with NE235H liquid scintillator, but without the phototubes mounted at the rear of each cell. In actual operation, the lucite front window shown here is replaced by a highly polished aluminum plate.

at Hope College. We expect the large detectors to be ready for use by the summer of 1982.

The signal-processing logic for the neutron detectors has been designed in detail, and involves a mixture of commercial NIM and CAMAC units with lab-built modules. The latter provide a) analog summing of pulse-height signals from various neutron-detector subcells, b) coincidence-latch logic to yield a firing pattern for the neutron-detector subcells, and c) neutron-detector readout control to transfer to the computer cell address, energy, and timing information for each subcell which is fired. Prototypes of the first two of these lab-built circuits have been fabricated and tested. All of the lab-built modules should be ready by summer, 1982.

Because of the large number of components involved in the neutron detector system, it is essential to have a reliable, light-pulsing diagnostic system to calibrate and monitor as a function of time, the pulse-height gain and effective threshold, the timing performance, and the electronic losses for all subcells. We have designed a system involving a high-power, externally triggerable, fast-pulse (width < 300ps) nitrogen laser. Beam expansion optics and wavelength shifting in a sample of the NE 235H liquid scintillator (included in a peristaltic-pump circulation system with the large detectors themselves) will allow illumination of every phototube through optical fibers embedded in the RTV "cookies" which optically couple the phototubes to the glass exit windows on the neutron-detector subcells. Construction and testing of this diagnostic system is now under way. Our eventual hope is to establish a closed-loop system, whereby changes in the response of specific subcells detected via the laser pulses will be fed back to the microprocessor-controlled high-voltage supplies (already in house) for the appropriate phototubes.

An additional development needed for application of the neutron detectors in the high-precision charge symmetry experiment is the implementation of a sophisticated Monte-Carlo code to simulate the detector response. A detailed understanding of the detector response (especially of any possible spin-dependence), to be attained from comparison of the Monte Carlo calculations with measurements, is crucial in assessing potential systematic errors that the detector may introduce in the measured left-right asymmetries between different beam-target spin combinations. We have written an appropriate Monte-Carlo code and are in the process of improving it. In addition to conventional calculations[3] of neutron detection efficiency resulting from n-p scattering and from a variety of n-^{12}C reactions induced in the scintillator, the code so far includes tracing of multiple interactions of a single neutron throughout the large-volume detector, asymmetries in the interaction of polarized incident neutrons with protons (but not yet with ^{12}C nuclei) in the liquid scintillator, and a realistic modeling of the light collection from any point within a given subcell.

1) S.E. Vigdor, IUCF Technical and Scientific Report, 1978 (p. 15); S.E. Vigdor et al., Proc. Fifth Intl. Symp. on Polarization Phenomena in Nuclear Physics (Santa Fe, August, 1980), edited by G.G. Ohlsen et al. (AIP, New York, 1981), Vol. II, P. 1455.

2) S.E. Vigdor et al., this Report, p. 52.

3) R.A. Cecil, B.D. Anderson, and R. Madey, Nucl. Instr. Meth. 161, 439 (1979).

(iii) Scintillator Hodoscope

The scintillator hodoscope to be used in experiment 93 ($n+p\rightarrow d+\gamma$)[1] been constructed and is undergoing diagnostic tests. The 46 cm by 30 cm active

area of this device is divided into 345 (23x15), two cm square cells by the 20 scintillator elements (twelve in the "X" axis and eight in the "Y").

To achieve this resolution each of the elements in an axis must partially overlap its neighbors and participate in the definition of three (two for end elements) axis positions. This scheme allows N elements to define 2N-1 positions. Each axis position requires that a particle traverse alternately 1 or 2 scintillator thicknesses but leaves no open areas through which the particle may pass undetected. For this device the elements are 1/8 inch thick, 6 cm wide (end elements 4 cm wide) and overlap their neighbors by 2 cm. Each element is viewed by an EMI 9826B photomultiplier tube.

An assembly language algorithom for determining the X and Y positions in the hodoscope has been written and is in on-line use as a RAQUEL sorting subroutine. Nonvalid events (zero or too many elements) are given locations outside the hodoscope's physical surface.

Because of the coincidence requirements of this system, noise and other incorrect events can produce distinctive position patterns.

1) H.O. Meyer et al., this Report, p. 57.

(iv) Scintillator Detector Lab

The Scintillator Lab has fabricated approximately 40 new detectors during the past year. These have included nearly all the plastic scintillators for the CSB project, a number of small detectors for the BL2 polarimeter, as well as a number of other counters for experimentalists.

Also, the Lab has repaired or modified a large number of existing detectors. This service is performed for both resident and visiting experimentalists.

(v) Multiwire Proportional Chambers (MWPC)

Several multiwire proportional chambers (MWPC), intended primarily for use with the charge symmetry breaking (CSB) experiment, have been designed, fabricated and tested at IUCF during the past year. Ultimately we will construct for CSB 6 small chambers of nominal 30 X 40 cm^2 active area, and 6 large chambers of nominal 65 X 90 cm^2 active area. The wire spacing for the small chambers is 1.95 mm and 2.54 mm for the "horizontal" and "vertical" position sensing chambers, respectively. Other specific (physical) features of these chambers follow general design considerations employed by the High Energy Physics (HEP) group at Indiana University.[1]

The chambers were fabricated at IUCF with the aid of a recently completed facility to aid MWPC construction. The facility includes equipment for making printed-circuit (PC) board layouts of a modest size (50 X 100 cm^2), and a large jig-plate "gluing table" (180 X 210 cm^2) for precision lamination of PC boards and other MWPC components. The actual wire winding for the MWPC has so far been carried out with a device built and used by the HEP group. For the present we have been able to fit into their scheduled use of the wire winder, but we may have to consider constructing such a device at IUCF to avoid future conflicts.

In order to record and interpret the hit pattern of wires for the MWPC, we are presently using a commercial MWPC readout system (LECROY-PCOSII), consisting of model 7700 MWPC chamber boards (nominal 600 ns delay) and an IUCF modified model 2700 (CAMAC) controller. There are 32 MWPC channels (16 hybrids) per board; each hybrid contains a dual amplifier, discriminator, delay, and latch in a single integrated circuit. For diagnostic purposes, we have constucted

the wire chambers in such a way that the readout for adjacent MWPC wires (e.g., odd versus even) is fed to alternate MWPC boards. Hence, bad hybrids, noisy boards, uneven discriminator settings, etc., result in different, yet characteristic, odd/even wire firing patterns, and this has proven to be invaluable for trouble shooting the MWPC system.

Tests of the above system and some preliminary CSB data taking runs have used the data acquisition program RAQUEL which accommodates the variable number of words/event associated with multiple "hits" in the MWPC's. At present, the program reads out up to 3-hit events for both an "x" and "y" MWPC, giving both the centroid and width for each hit (only information for the first encountered in the read-out sequence for multi-hit patterns in x or y), along with the total number of x and y hits. In principle much more information can be obtained from the MWPC encoder, although the above has been sufficient for all the initial tests.

After a shakedown test run with beam in July, the small x and y MWPC were used for two CSB runs, one in the beam swinger area in conjunction with a test of the prototype 12-cell neutron counter and one in the gamma cave where preliminary data on the analyzing power of the inclusive opening angle spectra for (p,2p) and (p,pn) were obtained.[2] These runs constituted the first use of a remote CAMAC crate at IUCF, which performed very well. The chambers themselves behaved reasonably well in these runs, operating in a plateau region (greater than 97% efficiency) at roughly -3 kV, with a position resolution equal to the nominal wire spacing. We have, however, experienced some problems with the MWPC boards and controller/readout system that we are at the present, in conjunction with LeCroy, attempting to resolve.

We have just recently finished construction of a prototype of the large area chambers to be used for CSB. In general, it is just a scaled-up version of the smaller chambers we have already constructed. However, instead of the aluminum-coated mylar cathode planes employed in the small chambers, the large prototype uses graphite coated mylar.[3] Because of its impedance (5-50 KΩ/square), it is hoped that the effects associated with rapid energy dissipation during sparking in such a large (high capacitance) MWPC should be reduced. Testing of this prototype chamber will begin shortly. If these tests go well, it is expected that all the MWPC needed for CSB will be constructed and ready for use by this coming summer.

In the meantime, design and prototypical detector construction will be starting for the detector systems to be used in the focal planes of the new double spectrometer system, and construction will begin in earnest during the latter part of the year.

1) R.R. Crittenden, S.C. Ems, R.M. Heinz, and J.C. Krider, Nucl. Instr. Meth. 185, 75 (1981).

2) S.E. Vigdor et al., this report, p. 52.

3) Acheson Colloids Co., Port Huron, MI 98060

(vi) Vertical Wire Drift Chamber (VWDC)

The VWDC has been used in several runs on the QQSP during the last year. By keeping the dark current at 1 microamp or less, the chamber was operated for 16 consecutive shifts. The problem of excessive dark current due to evaporation of protons from the target has been solved by the placement of an absorber plate in front of the drift chamber. Attempts to use a gas mixture of 49 1/2% Argon, 49 1/2% ethane, 1% ethyl alcohol failed because the plateau was too narrow for the type of electronics we are presently employing.

The electronics have not been finalized. Two

additional electronic systems are presently being evaluated.

In the past we have had trouble with occasional sparks shutting off the high voltage for the VWDC. This problem has been solved by using graphite cathodes.[1,2] A graphite cathode with a resistance greater than one kilo-ohm per square should limit the energy in a spark and keep the high voltage from shutting off. The graphite is, chemically, less active than aluminum and should last longer than aluminized mylar. The graphite cathode is made by spray painting Electrodag^R 154 on a mylar sheet.

The processing time of an event and the ultimate data acquisition rate using the VWDC are yet to be determined.

1) R. Hammarstrom et al., Nucl. Instr. and Meth. 174, 45 (1980)

2) M. Bozzo et al., Nucl. Instr. and Meth. 178, 77 (1980)

(vii) High-Purity Germanium Detector Telescope Systems

Operation of the high-purity germanium detectors has been routine since the discovery of the effect of radiation damage on their biasing characteristics, as reported last year. In 1981, these detectors were used in 14 different experiments without incident and detected particles ranging from 60 MeV protons to 200 MeV tritons and ^{3}He with spectral resolutions basically dominated by the kinematic broadening of the reactions. Examples of the use of the detectors in several experiments at IUCF are given in Figs. 7 and 8. Figure 7 is a spectrum for the ^{12}C(^{3}He,t) reaction using a 200 MeV ^{3}He beam, a 3.7 mg/cm^2 styrene target and a 3 element telescope containing 11mm and 15mm thick germanium detectors. The energy resolution is 400 keV and is primarily due to the kinematic energy spread of the beam.

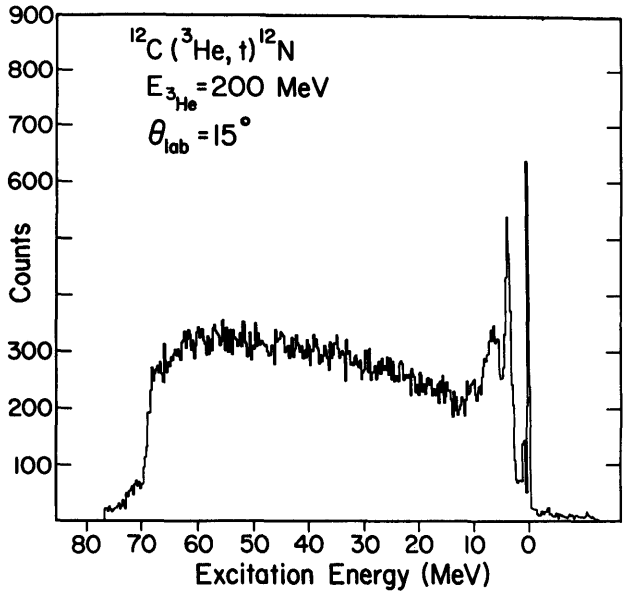

Figure 7. Excitation-energy spectrum obtained for the ^{12}C(^{3}He,t)^{12}N reaction using a germanium detector telescope.

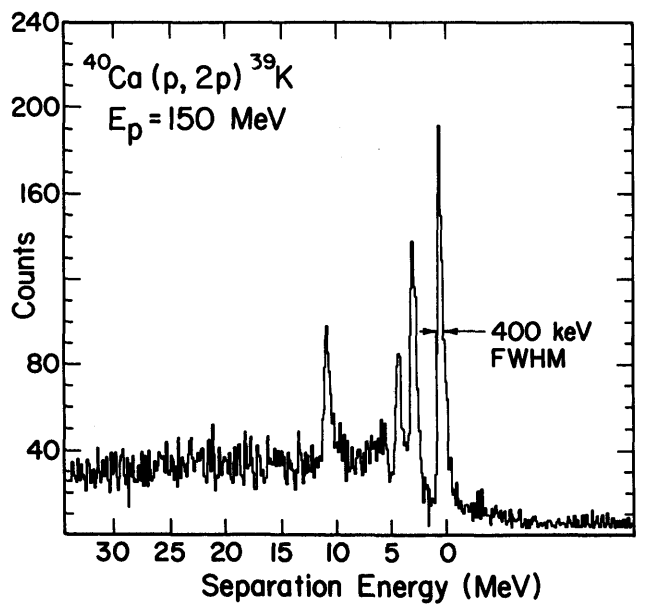

Figure 8. Summed-energy spectrum obtained for the ^{40}Ca(p,2p)^{39}K using two germanium detector telescopes.

Perhaps a better example of the utility of these detectors at intermediate energies is given in Fig. 8, which is a binding energy sprectrum for the ^{40}Ca(p,2p) ^{39}K reaction, where the two outgoing protons were detected in coincidence by two multi-element

germanium detectors. One telescope consisted of a 1mm thick silicon ΔE detector followed by a 14mm and a 15mm thick germanium detector, and was capable of stopping 116 MeV protons. The second telescope also contained a 1mm thick silicon detector and was followed by one 11mm and two 15mm thick germanium detectors. This telescope was capable of stopping 132 MeV protons. The incident proton energy was 150 MeV. The overall summed energy resolution was 400 keV, and was due largely to electronic noise in the preamplifiers. Nevertheless, these data represent the best energy resolution (p,2p) data yet taken by either particle telescopes or two arm magnetic spectrometers at intermediate energies.

While we have learned much about the use of these detectors, several questions about their properties in our environment remain to be answered. Foremost among these are the effects of radiation damage on the intrinsic resolution of the detectors for charged-particles. Generally, the beam energy spread and kinematic effects have masked any change in detector resolution so that no measurement has been made. To first order, then, the practical consequences of this effect on their use appears to be minimal. This needs to be verified.

Another concern was the possible variation in the charge collection efficiency of these detectors as a function of the particle range, similar to that reported for silicon detectors[1] and germanium detectors[2]. Preferential hole or electron trapping could cause such a variation -- radiation damage generates predominantly hole-trapping centers in germanium detectors[3]. If preferential hole trapping were to cause a variation in the charge-collection efficiency, the effect would be reversed when the particles are incident on opposite faces of the detector.

An experiment to specifically look for this effect was carried out at Indiana using a 60 MeV proton beam and a detector telescope, shown schematically in Fig. 9, consisting of a 10mm thick detector fabricated from N-type germanium, with 2mm thick silicon ΔE detectors mounted on either side. Scattered particles could then enter either face of the germanium detector by turning the cryostat around on the radial arm of the scattering chamber. The range of the most energetic protons, deuterons, and tritons from the ^{62}Ni (p,p'), (p,d) and (p,t) reactions which provide the energy calibration are shown in Fig. 9. There was no difference in the charge collected when the scattered protons, deuterons and tritons were incident on either face of the radiation-damage-free germanium detector, verifying our belief that this effect is not present in a "clean" detector. A similar test using a detector having a known measured amount of radiation damage also showed no change in the charge-collection efficiency as a function of ion detected.

A list of the existing high purity germanium detectors and their operating characteristics is given in Table I. Several new detectors are presently on order from the Lawrence Berkeley Laboratory and will be available sometime in 1982. These include two 2mm deep N-type detectors and one 2cm thick P-type stopping detector.

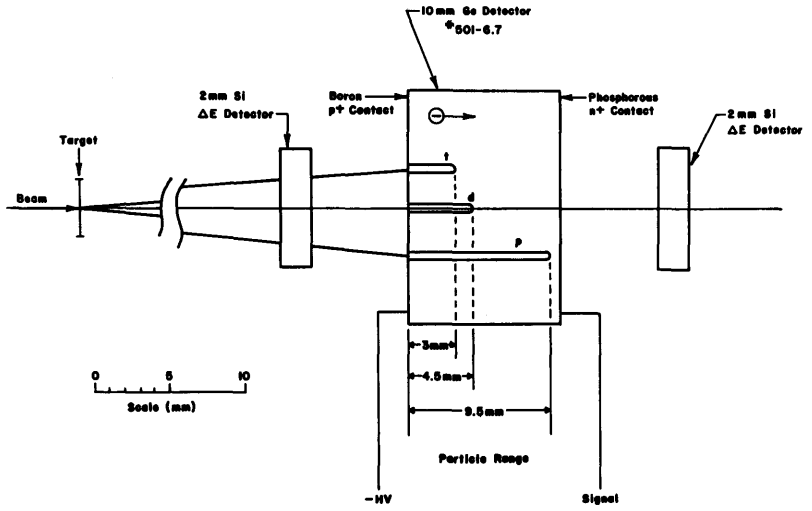

Figure 9. Schematic view of the germanium detector telescope system used to study charge collection efficiency.

TABLE I

Detector No.	Ge type	thickness (mm)	depletion Bias (-kv)	Delta (V)	Rad. Damage & Anneal Cycles	Thermal cycles	Total Anneal Time (hrs)	Li Layer Depth (mm)	Delivery Date
#172-3.1	p	10.6	600	>2000	>15	>17	>200	1.13	~1976
#514-7.0	p	15.21	1700	1300	13	50	752	1.59	3/21/77
#514-8.6	p	14.94	1450	1500	26	62	1073	1.10	3/21/77
#517-9.7	n	~15	1500	200	16	47	670	NA	8/15/77
#550-8.6	n	13.5	700	200	6	14	227	NA	11/30/79
#475-10.7	n	9.07	1700	300	4	22	216	NA	8/15/77
#501-6.7	n	10.77	1800	300	15	52	768	NA	8/15/77
#477-6.1	n	9.52	1750	150	0	2	3	NA	4/21/80
#551-11.8	n	5.18	1100	200	1	2	20	NA	4/21/80

1) K.W. Kemper and J.D. Fox, Nucl. Inst. Methods 105, 333 (1972).

2) G.M. Crawley, S. Gales, D. Weber, B. Zwieglinski, W. Benenson, D. Friesel, A. Bacher and B.M. Spicer, Phys. Rev. C 22, 316 (1980).

3) H.W. Kraner, R.H. Pehl, and E.E. Haller, IEEE. Trans. Nucl. Sci. NS-22, 149 (1978).

(viii) Target Lab Technical Status

The target lab supplied an estimated 95% of the targets used at IUCF in 1981. Targets prepared, in thicknesses ranging upward from 50 $\mu g/cm^2$, included: CD_2, $^{6,7}Li$, $^{7}LiCl$, ^{11}B, $^{12,13,14}C$, ^{24}Mg, $^{28,30}Si$, $^{28}SiO_2$, $^{30}SiO_2$, ^{31}P, $Na^{35}Cl$, $Ca^{37}Cl$, ^{34}S, ^{40}Ca, ^{39}KF, ^{51}V, ^{59}Co, ^{56}Fe, $^{58,60,61,62,64}Ni$, ^{74}Ge, ^{103}Rh, ^{116}Sn, $^{133}CsCl$, BaCl, $CeCl_3$, $^{144,154}Sm$, ^{166}Er, ^{185}Re, $^{186}WO_3$, ^{197}Au, $^{205}Tl_2O_3$, $^{207,208}Pb$, ^{209}Bi, $^{209}BiO_3$ glass, and $^{238}UF_4$. Most noteworthy, we were able to extend our grinding, settling and spraying techniques to produce 1 mg/cm^2 targets which gave ~40 KeV resolution.

Moving the lab to a much larger room was an ongoing major project for 2 1/2 months.

A new equipment addition is a R.D. Mathis vacuum evaporation thickness monitor. More controlled evaporation of many materials should now be possible. Work on the closed-loop glovebox continued; most of the customizing work on the box interior has been completed.

7. Data Acquisition System

(i) Data Acquisition Hardware

The past year has been spent in maintaining the three Harris computers, repairing our stock of NIM and CAMAC modules, and constructing and debugging electronics modules for the charge symmetry experiment. The hiring of one technician and one apprentice technician has brought the staffing level back up to its previous level.

The remote CAMAC system has been used successfully in several experiments. It provides ground loop isolation for a parallel branch highway at distances beyond 300 meters from the central computers.

The charge symmetry experiment has required the construction of special purpose hardware. In order to multiplex the 400 photomultiplier signals, eight analog summing modules and sixteen digital timing modules have been designed and built. Power supplies for the wire chamber cards and the photomultiplier tubes are in various stages of construction. The 4K FIFO event buffer and control logic modules have been designed but not yet constructed. The 3 CAMAC crate system will be controlled by dual PDP-11/23 processors. This development project will provide the prototype for a "smart" front-end for use with our future computer systems. This will allow high speed data transfers from the crates with a minimum of processing overhead on the host computer. (Initial measurements indicate a 24-bit data transfer every 10 microseconds is possible to achieve.)

(ii) Operating Systems

The DMS operating system has been stable during the past year; the only major change was to the FORTRAN compiler. The compiler was modified to enable the passing of arguments in the upper memory map (>64K). The SCOPE handler was modified to handle arrays from the upper map.

The VULCAN 9 system was installed. This seems to have solved some of the difficulties of previous versions, however several new problems were encountered. These new problems are known and there are simple ways around them. Therefore, VULCAN will be frozen at this level. The plotting programs were installed and are now in advanced stages of debugging.

(iii) Data Acquisition and Analysis Software

The major concentration of effort this past year was in the development of RAQUEL (Real time data AcQUisition and EvaLuation).

The concept of using dynamic core blocks has proven very successful from the point of view of software maintenance as well as eliminating arbitrary limits. One major restructuring was necessary in the

past year when it became evident that context switching between RAQUEL and the external sorting program was adding significantly to the software overhead in processing an event. The problem was solved by taking the interrupt driver event handling assembly software out of RAQUEL and putting it in the external sorting program. This had the additional benefit of enabling the relatively quick creation of individually tailored event handlers, e.g., a selective CAMAC reading on the basis of which bits are set in a coincidence register.

The concept of user maintained and created external sorting programs has proven very successful and many have been written by experimenters to acquire data from special detectors or to read data back from tape using user-chosen analysis routines. For the experienced programmer about five minutes is required to implement a common transformation. Users have also written external analysis programs to treat histograms to remove aberrations from magnetic detectors.

RAQUEL can now acquire from PACE and a special external sorting program has been written to optimize acquisition from the QDDM. In as much as the needs of the experiments which had complex event structures were met early in the year, some attention was then given to enhancing the data rate capability of RAQUEL. These efforts now manifest themselves by RAQUEL's being faster, in all modes, than DERIVE, the previous major acquisition system at IUCF. Using PACE in the spectrograph mode, a data rate of 14K words/sec is obtainable. This is the limit imposed by the hardware and system-interrupt handler.

A User Manual for RAQUEL has been written (IUCF Internal Report #81-7) and distributed. It contains a description of all commands, a recipe for setting up the acquisition software, a list of error messages and instructions for writing external sorting programs.

An external analysis program has been written (RAQPLT) to provide either default or specialized plots for the user.

The software controlled periodic alteration of the polarized beam spin state has been implemented and used.

The number of conditions which act as gates for histograms has been increased to enable jumps downward in the condition block. For example, if multiple 2-D windows are drawn on a histogram and these windows identify (say) protons, deuterons, etc., then if the event is within window 1 the test for window 2 is superfluous and can be bypassed by a JUMP entry in the condition block. The wide variety of conditions which can be utilized in constructing a gate for a histogram has proven to be a very powerful technique and sophisticated use has been made of them in complex on-line analysis.

B. Future Facilities

1. Polarized Neutron Beam Facility

This new experimental area is now nearing completion, as detailed below. We expect that in the spring of 1982 a proton beam will be brought down the primary beam line for initial room background tests with a solid neutron production target. Investigation of the properties of the neutron collimating system and measurements of the full neutron energy spectrum will follow with the availability of the liquid deuterium (LD_2) neutron production target. More detailed tests of the polarization and flux profiles of the neutron beam await calibration of a flux/polarimeter monitor with polarized beam. We expect that setup of experimental equipment in this area (multiwire chambers, large volume neutron counters, polarized proton target, etc.)

for the charge symmetry breaking (CSB) experiment[1] to be in full swing by the summer of 1982. From that time on, a relatively permanent setup of target/detector/electronics for CSB will occupy this space until the completion of data acquisition for this experiment.

The layout of the polarized neutron facility (PNF) is complete and, with the exception of some additional shielding for the neutron collimator and the large volume scintillator detectors, the configuration of the shielding walls and primary beam line components exists as indicated in the overview of the area in Fig. 10. All additional special shielding has been fabricated and awaits final placement. Neutron shutters for both the PNF and QDDM areas have been installed in the primary radiation shielding wall and the radiation interlock system has been suitably updated. The shielding wall near the CSB dump has been positioned so as to make way for the eventual constuction of the dual spectrometer system in the far north high bay area.

A more detailed layout of the beamline is given in Fig. 11. The incident proton beam is focussed by a quadrupole doublet and deflected down by a 10° bending

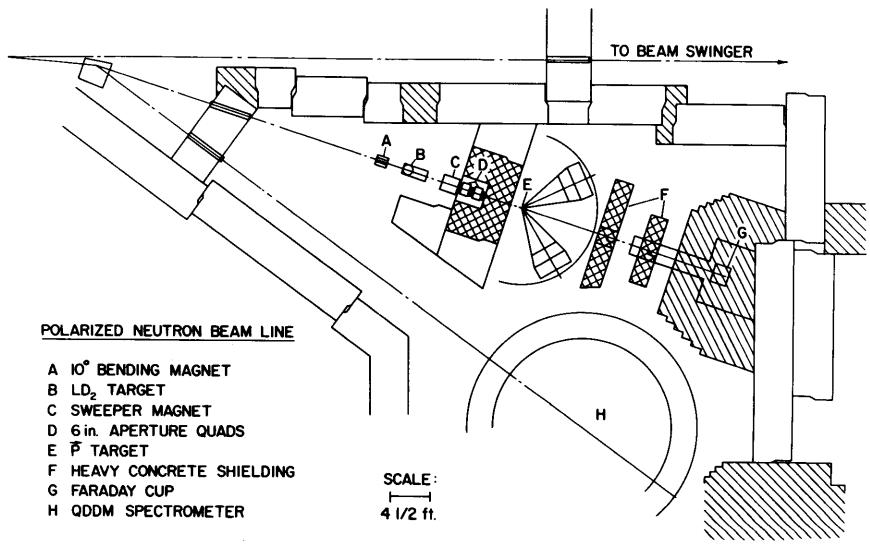

Figure 10. Floor plan of the polarized neutron beam line area.

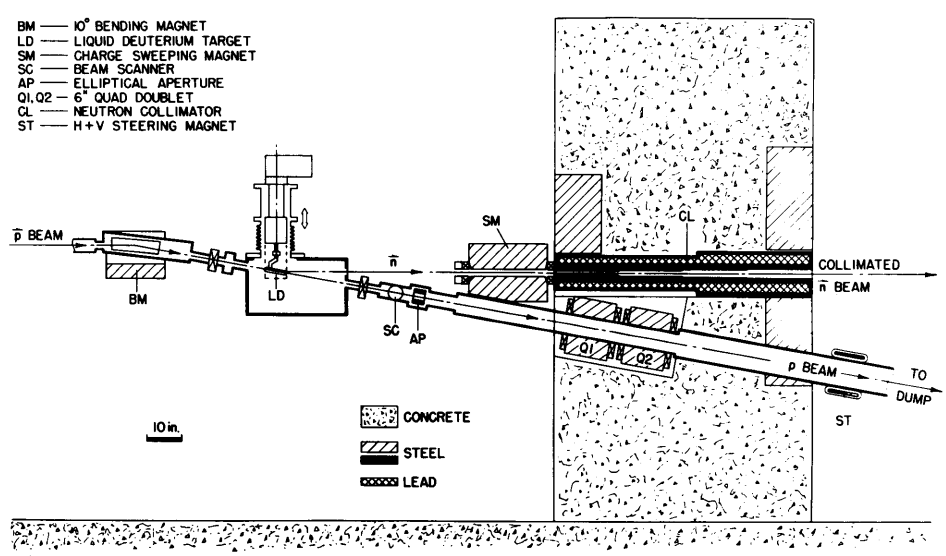

Figure 11. Side view of the polarized neutron beam line.

magnet to form a 4 X 4 mm^2 beam spot on the 20-cm long LD_2 neutron production target. The exit line for the primary proton beam has a scraper (intercepting on the order of 1% of the multiply-scattered beam), and a large aperture (15 cm diameter) quadrupole doublet to focus the beam into a well-shielded beam dump about 12 meters from the production target. The dump contains a 4-sector split Faraday cup 0.3 m below the floor level, which feeds signals back to a pair of large-aperture x-y steerers, in order to keep the beam centered in the cup. Additional beam monitors will provide appropriate diagnostic information to keep the beam aligned and centered on the LD_2 production target.

The neutrons exit the production target and the target vacuum enclosure parallel to the floor (i.e., at a 10° reaction angle from the primary beam) through thin Kapton windows. The "neutron beam" then passes through a 0.5 Tesla-meter charged particle sweeping magnet about 1.6 meters from the LD_2 target. The sweeping magnet will incorporate a 50-cm long lead pre-collimator for the neutrons. The horizontal and vertical extent of the resulting beam is determined by the size of a 1.9-meter long lead- and steel-lined collimator built into the collimator shielding wall which follows the sweeping magnet. The wall itself serves as an anti-scattering aperture for the collimator and includes about 0.6 meter of steel plus 1.3 meters of heavy concrete (corresponding to about 6 mean-free-path lengths for 200 MeV neutrons). The neutron beam size at the polarized proton target position, 4.25 meters from the production target, will be approximately 6 cm wide by 8 cm high. The total flux of neutrons for all energies up to 200 MeV incident beam energy, for about 50 na of primary beam, is expected to be about 10^5 n/sec/cm^2. Approximately half of these neutrons will be in the charge-exchange peak $E_n \cong$ 170-200 MeV. The large spectral broadening arises mainly from energy loss in the production target.

The polarization transfer in the charge-exchange reaction D(p,n)2p near 10° at 200 MeV is nearly complete for the transverse beam polarization component in the vertical reaction plane. Adopting average values of $R_t = -0.85$ and $A_t = -0.1$ from recent n-p phase shifts,[2] we expect the neutron polarization to be $P^n_y = 0.6$ for an incident proton polarization of $P_o = 0.75$. A small component of neutron polarization in the horizontal plane (of order 0.1 P^n_y) arises from the longitudinal polarization component introduced into the primary beam by spin precession in the 10° bending magnet; see Fig. 12 for a detailed presentation of the various polarization components and their calculation.

Vacuum enclosures, special beam-line diagnostic devices, and stands for the various beam-line

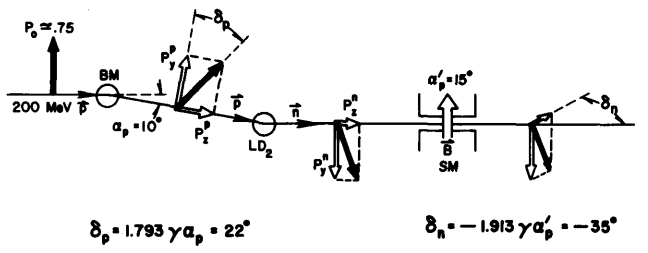

$$\begin{cases} P^p_y = P_o \cos\delta_p = .927\,P_o \\ P^p_z = P_o \sin\delta_p = .375\,P_o \end{cases}$$

$$\begin{cases} P^n_y = P^p_y R_t + P^p_z A_t = -.80\,P_o \simeq -.60 \text{ for } R_t \simeq -.85,\ A_t \simeq -.1 \\ P^n_z = P^p_y R'_t + P^p_z A'_t = +.08\,P_o \simeq .06 \quad \text{for } R'_t \simeq .05,\ A'_t \simeq .1 \end{cases}$$

$$P^n_z \text{ rotated by } \delta_n \Longrightarrow \begin{array}{l} P^n_x = -.04\ P_o \simeq .03 \\ P^n_z = .07\,P_o \simeq .05 \end{array}$$

Figure 12. Polarization vectors (dark arrows) and longitudinal or transverse components (light arrows) for polarized neutron production set-up, showing spin orientations of p beam before production target (LD_2) and n beam after target and sweeping magnet (SM).

components have been constructed and are presently being installed on the floor. The special beam-line magnets, large-aperture quadrupoles, and 10° bending and sweeper magnets (obtained commercially) have undergone tests and field measurements at IUCF. The neutron collimator system has been designed and fabricated and is ready for installation and alignment. We have finally acquired (thanks to the Universities of Maryland and Illinois) enough steel to complete the beam dump and neutron collimator shielding wall. This work is now in progress. Final assembly of the split Faraday cup has begun.

The cryostat, gas-handling and safety-venting system needed for the LD_2 production target have been developed and used successfully in an experiment employing a liquid hydrogen target to study the n-p capture reaction.[3] Modifications for use of the target in the PNF beam line, including additional safety interlock requirements, and construction of a target motion assembly for target in/out measurements, are underway. Since the application in the PNF requires that the LD_2 operate directly in the beam-line vacuum, a fast-acting valve is being purchased in order to prevent deuterium from dispersing into the other experimental area beam lines or the main cyclotron tank, in the event of an accidental rupture of the target.

1) For futher details, see page 52 of this Report.
2) R.A. Arndt et al., Phys. Rev. C15, 1003 (1977). 3.
3) See page 57 of this Report.

2. Indiana-Maryland Dual Spectrometer System

Funding was obtained from the NSF in September of 1981 to initiate construction of a two spectrometer system for IUCF. The larger spectrometer is the responsibility of the Indiana group and is optimized for high resolution spectroscopy. The design goal is 10 keV fwhm from the spectrometer (15 keV overall in the experiment) with an energy bite of at least 20 MeV (range of excitation energies on the focal plane detector) for all energies from 80 to 200 MeV. These goals are met in the completed design for a solid angle in excess of 6 msr for particles of maximum rigidity 3.6 Tesla-meter (288 MeV deuteron kinetic energy) at a field of 1.64 Tesla. The focal plane is 4 by 80 cm with position and angle measurement in the bend plane to a precision of 0.16 mm (perpendicular to the flight path) and 3 mrad fwhm. The orthogonal position is measured to 5 mm precision fwhm as a guide to setting the entrance quadrupole field but is not normally required in aberration correction to meet the resolution goals. The first 55° dipole weighs about 50 tons and has a gap of 10 cm. The beam fills the gap at the entrance but is sufficiently reduced in size at the exit to leave room for a pole face correction coil for changing the effective exit curvature to set the (x/θ^2) aberration to zero at one point on the focal surface for each of the three dispersion modes. The second 60° dipole weighs approximately 70 tons with an 8 cm gap, again filled by the beam envelope at the entrance but provided with a triangular pole-face winding near the middle permitting kinematic correction [up to $K = \pm 0.05$, where $K = 1/pdp/d\theta$] at maximum field. Each dipole requires 80 kW with coils matched to power supplies provided by the Maryland group. The entrance quadrupole has a 20 cm gap and departs from pure four-fold symmetry to introduce hexapole and octupole corrections which minimize (x,ϕ^2) and $(x,\theta\phi^2)$ contributions to the resolution. Both spectrographs use the same quadrupole design.

The second spectrometer is the responsibility of

the Maryland group and is optimized for a maximum product of solid angle and momentum range with moderate resolving power ($p/\Delta p \sim 2000$). The completed design has a solid angle in excess of 13 msr with a momentum coverage $P_{max}/P_{min} = 1.356$ up to 2.53 Tesla-meters (269 MeV protons) at 1.7 Tesla. The focal plane detector is 85 by 16 cm and requires position and angle determination of 0.9 mm and 18 mrad fwhm in the bend plane and 4 mm resolution in the transverse plane. The split 70° dipole weighs about 40 tons and requires 90 kW.

In single arm experiments with the 3.6 Tm spectrometer, the 2.5 Tm spectrometer serves as a superb monitor not only of the luminosity (product of beam current and target thickness) but also of spot size and position on the target. In particle coincidence experiments the configuration of one spectrometer horizontal and the other vertical gives a complete measurement to high precision of both in-plane and out-of-plane momentum components.

3. The IUCF Cooler Ring

In a typical IUCF experiment a beam of a fraction of 1 μA is passed once through a target of thickness on the order of 10 mg/cm^2 and then stopped in a well-shielded beam dump. The probability of a nuclear reaction by a beam ion with a target nucleus is about 10^{-5}; nearly all of the beam contributes only to the room background, setting an upper limit to the targeted beam current which the detectors will tolerate and a lower limit to the cross section which is observable. The target thickness limit is set by the deterioration of beam quality through small-angle Coulomb scattering by the target nuclei and/or energy straggling caused by the target electrons.

If the beam were to be injected into a storage ring, the circulating current at the same emittance

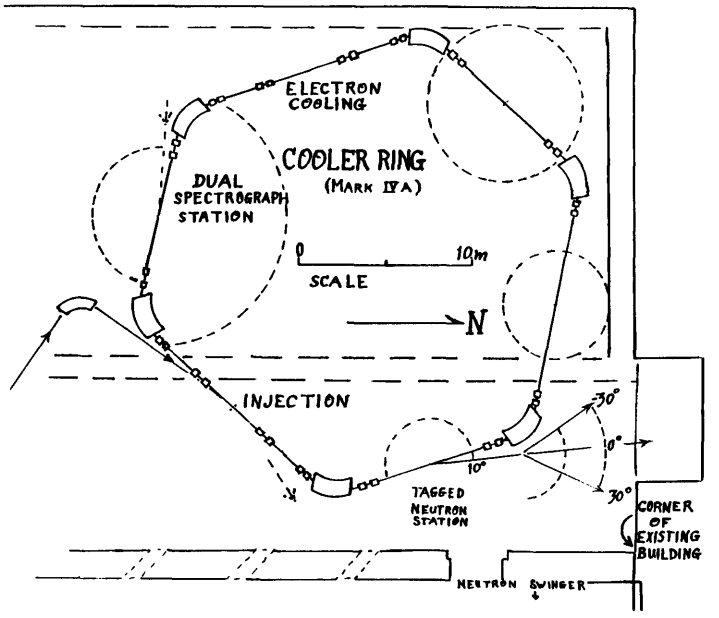

Figure 13. Layout of the Cooler ring showing dual spectrograph system and tagged neutron station located at two of the target waists. The ring will be located in an addition to the northwest corner of the present building.

could be larger by a factor 10^4 or 10^5, so that the average target thickness could be reduced by the same factor and still yield the customary luminosity (current-target thickness product). Of course after many traversals the beam quality will deteriorate in the identical fashion so that nothing is gained except for a non-trivial subset of experiments with a heavily ionizing product. If the target is thin enough, however, the beam will survive in the ring long enough that certain "beam cooling" processes can be employed to remove the incoherent velocity components being introduced by the target. A thermal equilibrium may be established between the "beam heating" by the target traversals and the simultaneous beam cooling elsewhere in the ring. The fastest cooling process now known is accomplished by immersing the ion beam in a cold comoving intense electron beam during a portion of each revolution. Cooling times on the order of 0.1 second are possible. Calculations show that for a light ion beam at IUCF energies the equilibrium may be

established for target thicknesses averaging less than 1 mg/cm^2 and that the beam will then survive for seconds to minutes depending on target Z with the dominant loss mechanism being nuclear interactions with the target and the probability of loss by nuclear reaction being about 10^{-1}. Luminosities are comparable to one-pass experiments with milligram/cm^2 targets. However the background is reduced in proportion to the increase in beam usage efficiency, i.e. by factors of 10^3 and more.

If the target thickness is further reduced, the stored beam becomes colder with the maximum decrease in emittance being on the order of the ratio of ion to electron masses. This beam quality is much superior to that which is available from any existing accelerator and promises greatly increased resolution in selected experiments.

At the end of 1980 IUCF submitted a proposal[1] to the NSF for construction of a "Cooler" (beam storage ring with electron cooling) and a "Tripler" (3.6 Tesla-meter booster cyclotron to expand the IUCF energy range). The cooler geometry was configured to give good experimental access to two target waists, one being at the target location of the new dual spectrometer system described elsewhere in this report.

It has been decided that the project should be undertaken in phases, with the Cooler to be constructed as rapidly as possible and the Tripler deferred for the present. During 1981 a variety of Cooler configurations has been investigated, including six-sided rings with experimental access to 3 or 4 target waists. Architects have prepared a building addition design to be located along the west wall of the present building and bonding authority is being sought from the State of Indiana so that construction may begin. The building is designed to provide space both for the Cooler and later the Tripler.

On the present time schedule, Cooler construction may begin at the start of calendar 1983 and be completed during 1986.

In this brief summary it has not been possible to describe the numerous other experimental advantages of stored beam experiments such as polarized beams on pure polarized targets, variable time structure including pure DC beams, energy ramping, tagging, recoil analysis, use of the ring as detector for total cross sections or as absolute energy calibrator by induced depolarization. Because the ring experiments use the beam so efficiently, the cyclotron beam is available for other users most of the time so that long duration experiments become feasible. The interested reader is referred to the 1980 proposal for a discussion of the scientific motivation and for more technical detail.

[1]The IUCF Cooler-Tripler: proposal for an advanced light-ion physics facility" December 1980.